

Article

Not peer-reviewed version

Design of Alternatives to Stained Glass with Open-source Distributed Additive Manufacturing for Energy Efficiency and Economic Savings

Emily Bow Pearce , [Joshua M. Pearce](#) , [Alessia Romani](#) *

Posted Date: 29 May 2025

doi: 10.20944/preprints202505.2332.v1

Keywords: stained glass windows; additive manufacturing; 3D printing; distributed manufacturing; energy efficiency; polycarbonate; economic analysis; Design for Additive Manufacturing (DfAM); Open design; Open source hardware



Preprints.org is a free multidisciplinary platform providing preprint service that is dedicated to making early versions of research outputs permanently available and citable. Preprints posted at Preprints.org appear in Web of Science, Crossref, Google Scholar, Scilit, Europe PMC.

Copyright: This open access article is published under a Creative Commons CC BY 4.0 license, which permit the free download, distribution, and reuse, provided that the author and preprint are cited in any reuse.

Article

Design of Alternatives to Stained Glass with Open-Source Distributed Additive Manufacturing for Energy Efficiency and Economic Savings

Emily Bow Pearce ¹, Joshua M. Pearce ^{1,2} and Alessia Romani ^{1,*}

¹ Department of Electrical & Computer Engineering, Western University, 1151 Richmond St. N., London, ON N6A 3K7, Canada

² Ivey Business School, Western University, 1151 Richmond St. N., London, ON N6A 3K7, Canada

* Correspondence: aromani2@uwo.ca

Abstract: Stained glass has played important roles in heritage building construction, however, conventional techniques of fabricating it have become economically prohibitive due to both capital costs and energy inefficiency. To overcome these challenges, this study provides a new design methodology for customized 3D printed polycarbonate (PC)-based stained-glass window alternatives using a fully open-source toolchain and methodology. This procedure involves fabricating an additional insert made of (i) a PC substrate and (ii) custom geometries directly 3D printed on the substrate with PC-based 3D printing feedstock (iii) to be painted after the 3D printing process. This alternative is intended to be used instead of traditional stained glass or, better, in addition to conventional windows to provide stained-glass design patterns while improving thermal insulation. Three approaches are developed and demonstrated in this study to generate customized painted stained-glass designs using (i) online-retrieved 3D and 2D designs; (ii) custom designs, i.e., hand-drawn and digital-drawn images; and (iii) AI-generated designs. The proposed methodology shows potential for distributed and accessible applications in the building and heritage sectors, especially for the repair and replication of existing conventional stained glass and the design of new customizable products that are 50 times less expensive than traditional stained glass.

Keywords: stained glass windows; additive manufacturing; 3D printing; distributed manufacturing; energy efficiency; polycarbonate; economic analysis; Design for Additive Manufacturing (DfAM); open design; open source hardware

1. Introduction

Born as an artistic decorative technique, stained glass played important historical roles in building construction [1], particularly for heritage buildings. This technique traditionally involves colored glass compositions assembled into complex patterns or pictorial drawings using metal-based striped frames, known as comes, overcoming the initial technical and economic limits in producing large glass laminates in the Middle Ages [2]. Current stained glass fabrication has changed according to the technological advancements in material production and manufacturing, generating different techniques and variations, e.g., Tiffany glass or painted stained glass [3,4]. These advancements have paved the way for digital fabrication tools, e.g., CNC-cutting [5], connecting artistic skills and crafts with industrial design and engineering. Widely adopted for Western European cathedrals in the 12th century [6], stained glass windows have been used in different sectors, ranging from decorative window elements to product artifacts [7]. Its applications are currently connected to (i) religious buildings, e.g., churches, synagogues, mosques, and temples; (ii) cultural and public buildings, e.g.,

transportation stations, libraries, or theaters; (iii) residential buildings, e.g., private houses and rooms; and (iv) interior and product design elements, e.g., mirrors and lamps.

From the literature, most works have focused on the study of historical stained glass, e.g., physical and chemical analyses [8,9], their alteration due to aging, atmospheric environment, and micro-organism action [10,11], or their restoration and conservation techniques [12,13]. In contrast, very few studies have considered the environmental and economic aspects of stained glass in current building applications, as well as potential alternatives through new fabrication methods [14]. Although more than half of heat loss through the outer surface of buildings can be attributed to glazed areas, substantial progress has resulted in window technology to help reduce this energy loss [15]. These technical advancements that can improve building efficiency have focused on conventional windows [16], excluding specialty windows, such as stained glass. For example, many churches, especially in Europe, were originally constructed without heating systems, but now, heating such large and normally uninsulated buildings is economically prohibitive [17]. Stained glass alone is energy inefficient in heating environments, as it tends to be single glazing and has metal comes running through the entire width, which are good thermal conductors [18]. In heritage buildings, one approach to improving energy efficiency is to replace windows [19], e.g., replacing single-glazed windows with double-glazed windows [16]. A similar approach for retrofitting stained glass in heating environments includes adding single or double-glazed protective glazing, which is generally inserted on the exterior to protect the stained glass and reduce heat loss [17]. These approaches are effective but rely on existing stained glass structures. Adding stained glass windows to new buildings or fixing existing ones is expensive. The national average cost for new stained glass in the U.S. is US\$ 6,372/m² (US\$ 592/ft²) and ranges from US\$ 3,380 to US\$ 9,558/m² (US\$ 314 to US\$ 888/ft²) [20,21]. Similarly, repairing stained glass costs between US\$ 969 and 10,226 per m² (US\$ 90 to US\$ 950/ft²), with the average cost being US\$ 4747 per m² (US\$ 441/ft²) [22]. These costs add up quickly, as religious and public buildings, in particular, can have expansive window areas. For example, a single church in Chartres has more than 2,000 m² (about 21,500 ft²) of stained glass [23]. Thus, replacing all of the stained glass would cost US\$ 12.7 million at the average rate.

It should also be pointed out that stained glass can improve energy efficiency in hot environments. Its use can effectively reduce solar transmittance and, thus, solar heat gain to reduce cooling loads of buildings in summer [24] and cooling-load-dominated environments [25]. Unfortunately, the cost of stained glass is generally prohibitive in cooling-load-dominated developing regions near the equator as well. This fact limits its real adoption in specific geographical and socio-economic contexts, lacking accessible and suitable alternatives.

Therefore, a means to provide the aesthetic and functional customization of stained glass is needed, allowing for the selection of energy-efficiency properties (e.g., optical properties to reduce heat gain) while reducing the cost and, ideally, increasing thermal insulation. To this end, one promising approach to reducing costs in glazing is to use polycarbonate (PC) [26] as an alternative material, which offers good impact and shattering resistance, lightweight, cost-effectiveness, and thermal insulation. Typical manufactured raw materials for buildings are coextruded PC multi-sheet systems with chambers for insulation and UV-resistant coatings to protect them from aging [26].

In addition, a new approach to manufacturing processes that has consistently reduced costs is distributed manufacturing. Among those, additive manufacturing (AM) processes further enlarged the possibility of manufacturing small batches of customized parts at local levels [27–29], especially following open-source, Design for AM (DfAM) [30], and open-design principles [31]. For example, prosumers could justify the cost of an open-source self-replicating rapid prototyper (RepRap)-class 3-D printer [32,33] by 3D printing only one object a week and earning a 100% return on investment after five years [34]. There is some evidence that this transition to distributed AM is underway [35]. This fact means that distributed AM could also be applied to PC feedstock. Filament-based 3D printing, i.e., fused filament fabrication (FFF), with PC alone [36] and in mixtures is already common and well-characterized [37,38] and can even be done from scrap PC granular waste directly thanks to fused granular fabrication (FGF) [39,40]. Moreover, AM technologies have already been used to

replicate complex images and 2D models as 3D-printable 3D geometry, converting existing images into Standard Triangle Language (STL) files or 3D printing paths for gcode generation [41–43]. Nevertheless, similar approaches for energy efficiency applications in the building and heritage sectors are still unexplored despite the potential economic and environmental benefits.

This study investigates the use of open-source material extrusion additive manufacturing to make customizable polycarbonate-based stained glass alternatives for the building and heritage sectors. It provides a new design methodology for 3D printed polycarbonate-based stained-glass window alternatives following open design principles, using a fully open-source toolchain and methodology. The proposed DfAM methodology aims to reduce the cost of new stained-glass design elements and solve the energy efficiency issues with historic buildings using stained glass, allowing for accessible custom stained-glass parts. This procedure involves fabricating an additional PC insert made of (i) a PC sheet as a substrate and (ii) a custom geometry directly 3-D printed on the substrate with PC 3D printing feedstock (iii) to be painted after the 3D printing process. This alternative is intended to be used instead of traditional stained glass or, better, in addition to conventional windows to provide stained-glass design patterns. Three approaches are developed and demonstrated in this study to generate customized painted stained-glass designs using (i) online-retrieved 3D and 2D designs; (ii) custom designs, i.e., hand-drawn and digital-drawn images; and (iii) AI-generated designs. After presenting the methodology and manufacturing results, an optical spectrum characterization and transmission analysis were performed on the painted surfaces to quantify the potential heat gain reduction, as well as a preliminary economic analysis in the context of low-resource settings.

2. Materials and Methods

The methodological workflow of the experimental 3D-printed polycarbonate-based stained-glass window alternatives followed five steps (Figure 1):

1. Selection or design of the 2D images for the final stained-glass designs, e.g., sketches, drawings, raster, or vector images (Subsection 2.1, Figure 2).
2. Conversion of the 2D images and creation of the 3D models saved in mesh format, i.e., STL (Subsection 2.2).
3. Slicing of the 3D mesh models and generation of the gcode files (Subsection 2.2, Figure 3).
4. Fabrication of the PC-based 3D design on the PC substrate via FFF 3D printing (Subsection 2.3, Figure 4).
5. Manual coloring of the 3D-printed PC inserts through acrylic painting techniques (Subsection 2.3, Figures 7-10).

These steps were all completed with an open-source toolchain made up of free and open-source software [44] and open hardware [45], following the principles of open design for the whole process [31]. In addition, optical spectra and transmission characterizations were carried out after the fabrication and painting steps (Subsection 2.4), and a preliminary capital cost economic analysis was performed (Subsection 2.5). The 2D images, 3D mesh models, 3D printing profiles, and gcode files of the different sample designs are available in the OSF repository [46].

PC-based Stained Glass 3D printing (Open-source tool chain and methodology)

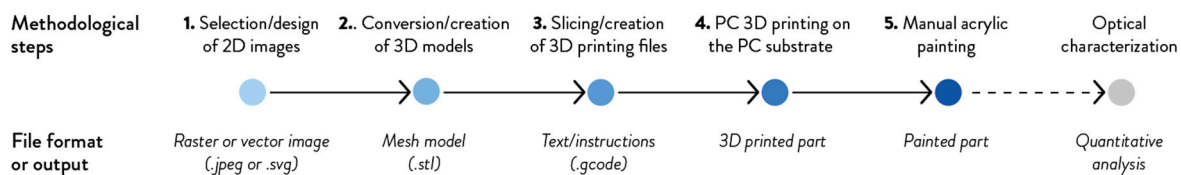


Figure 1. Methodology and workflow of the experimental work divided into five main design and manufacturing steps (Steps 1-5), reporting the corresponding file format and output, followed by optical characterization for quantitative analysis.

2.1. Phase 1: 2D Image Selection and Design

Three approaches were demonstrated to generate customized paint stained-glass designs for 3D printing starting from 2D raster or vector images, such as Joint Photographic Experts Group (JPG) or scalable vector graphics files (SVG). Six different designs and samples were generated accordingly (Figure 2), which means:

1. Online-retrieved 3D and 2D designs: collected designs made up of 3D models, i.e., sample stained-glass window from GrabCad (Figure 2a), and 2D vector images, i.e., logo from Appropedia (Figure 2b), both available on the Internet.
2. Custom designs, i.e., digital-drawn and hand-drawn images: novel custom designs from a digitally hand-drawn image (Northern Lights, Figure 2c) and a digital acquisition of a pencil sketch (Viking ship, Figure 2d), saved as vector images.
3. AI-generated designs: novel custom design from an AI image generator (Angel, Figure 2e), saved as raster image and converted into vector.

Finally, an additional vector image of a rectilinear geometric shape was made to quantify the total light transmission of PC-stained glass windows obtained following the proposed methodology (Figure 2f). The specifications of the six designs are summarized in Table 1. Each sample design image was made or modified considering square PC sheets with a 92900 mm² (1 ft²) area and a maximum 3D printable volume of 254 × 254 × 1.3 mm (10 in by 10 in × 0.05 in) for the 3D printed sample parts.

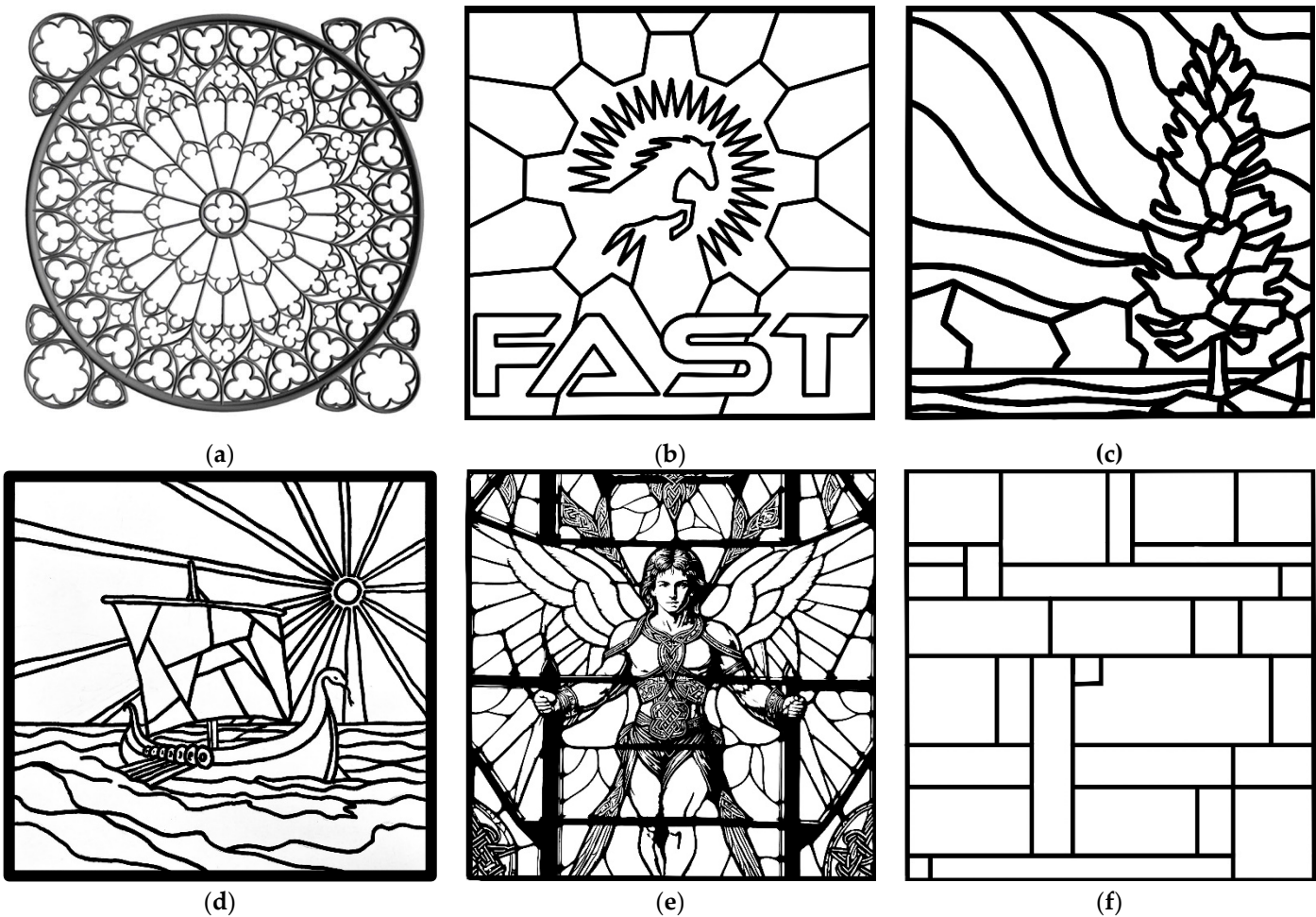


Figure 2. JPG and SVG images for the sample designs: (a) Notre Dame Rose Window (SG01); (b) FAST logo (SG02); (c) Northern Lights (SG03); (d) Viking Ship (SG04); (e) Angel (SG05); and (f) Geometric calibration pattern (SG06).

Table 1. Specifications of the stained glass designs used for this experimental work, highlighting the design category, the origin of the 2D design, the used file formats for 3D printed stained glass designs (image, 3D model, and 3D printing file).

Sample and nomenclature	Design Category	2D design (origin)	Image format	3D model format	3D printing format
Online Notre Dame Rose Window [47] - SG01	Online designs (Section 2.1.1)	Retrieved design (3D model, online)	SVG (vector)	STL (mesh)	gcode
Online FAST Logo [48] - SG02	Online designs (Section 2.1.1)	Retrieved design (2D image, online)	SVG (vector)	STL (mesh)	gcode
Digital Created Northern Lights-SG03	Custom designs (Section 2.1.2)	Digital drawing	SVG (vector)	STL (mesh)	gcode
Viking Boat - SG04	Custom designs (Section 2.1.2)	Paper drawing (digital acquisition)	JPEG (raster)	STL (mesh)	gcode
AI created Angel - SG05	AI-generated designs (Section 2.1.3)	AI-generated image	JPEG (raster)	STL (mesh)	gcode
Digital Created Geometric - SG06	Geometric validation (Section 2.1.4)	Digital Image	SVG (vector)	STL (mesh)	gcode

2.1.1. Online-Retrieved Designs

A classic design already digitally available as a 3D mesh model was selected as a first sample design (SG01), i.e., the Rose Window on the Notre Dame Cathedral [47] (Figure 2a). This 3D model has an overall height of 10 mm, which can cause warping of thin PC sheets during the 3D printing and is not required for 3D-printed stained glass fabrication. For these reasons, this 3D model design was processed as a 2D image, as would most other 3D designs found on the Internet not specifically made for this application. A vector logo design was selected as a second sample design (SG02) from already available images, i.e., the Western University Free Appropriate Sustainability Technology (FAST) Laboratory logo [48] (Figure 2b). In both cases, images were processed using the open-source raster graphic image editor GNU Image Manipulation Program (GIMP) [49]. They were cropped, and the color was removed using a paint bucket and auto-select tools, so the images were converted into black and white images and then saved as raster JPG files. The images were then imported into the open-source vector graphic image editor Inkscape (Inkscape, Boston, Massachusetts, U.S.) [50], where they were turned into vectors and saved as vector SVG files by using the “Trace bitmap” option according to the parameters shown in Table 2. This conversion into vector formats allows for high-quality images with better scalability, defined lines, and edges when resized according to the substrate dimensions, and easy to edit and manipulate them in 3D modeling and CAD software.

Table 2. Parameters for the “Trace bitmap” option in Inkscape for the conversion of raster into vector images for the stained glass 3D printing process.

Parameters for Bitmap Creation	Value
Detection Mode	Autotrace
Filter Iterations	4
Error Threshold	2.0
Speckles	1000

Smooth Corners	1.000
Optimize	0.000

2.1.2. Custom Designs: Digital-Drawn and Hand-Drawn Images

Digital drawings were prepared for the third sample design (SG03) using the open-source painting software Krita [51]. The digitally hand-drawn image of the Northern lights was saved as a JPG file. Then, it was imported into Inkscape and turned into a vector SVG file (Figure 2c) by creating paths with the same settings as in Table 2.

A hand drawing of a Viking ship was completed on paper with a graphite pencil for the fourth sample design (SG04). It was retraced with a Sharpie marker to make the lines more visible for digital acquisition and match the stained glass aesthetics and formal language. The drawing was then photographed with a camera phone and saved as a JPG file. Using GIMP, the image was cropped and edited to make it monochromatic as well as improve the contrast and maximize the black point high, increasing the accuracy of the vector conversion. As for the previous designs, it was then processed into a vector SVG file (Figure 2d) using the parameters summarized in Table 2.

2.1.3. AI-Generated Design

The AI-generated image was created as a fifth sample design (SG05) using the open-source generative AI software Stable Diffusion A1111 [52] with the prompt for a clear stained glass image of an angel. The raster JPG image was then turned into a vector SVG file (Figure 2e) by creating paths with Inkscape with the same settings as in Table 2.

2.1.4. Geometric Validation Image

A rectilinear geometric shape image with known rectilinear sizes, 254 x 254 mm, was created as a sixth sample design (SG06) to validate the whole methodology. This validation image was intended to calculate the total transmission of a stained glass window with different colors and shapes through the open-source software ImageJ [53]. Consistent with the earlier designs, the design was next processed into a vector SVG file (Figure 2f) using the parameters detailed in Table 2.

2.2. Phases 2 and 3: Creation of the 3D Mesh Models and 3D Printing Slicing

The SVG files of the six sample designs were imported into the open-source slicing software Prusa Slicer v 2.9.0 (Prusa Research, Prague, Czech Republic) [54] and scaled down to the size requirements of the experimental 3D printable PC sheets, i.e., 254 × 254 × 1.3 mm. The main 3D printing slicing settings and parameters of the sample designs are summarized in Table 3. They were sliced to a maximum height of 1.3 mm to prevent warping and match the aesthetic and formal language of stained glass. They were then exported as gcode files and STL files (Figure 3) for the 3D printing process.

Table 3. 3D printing parameters for polycarbonate printing on top of polycarbonate sheets.

3D printing parameter	Unit	Value
Nozzle Diameter	mm	0.8
3D printing temperature	°C	245
Build Plate Temperature	°C	105
3D Printing Speed	mm/s	60
3D Printing Speed (initial layer)	mm/s	30
Extrusion Flow	%	100
Number of Perimeters	//	3
Layer Height	mm	0.8
Layer Height (Initial layer)	mm	0.5

Number of bottom/top layers	//	3
Infill percentage	%	100

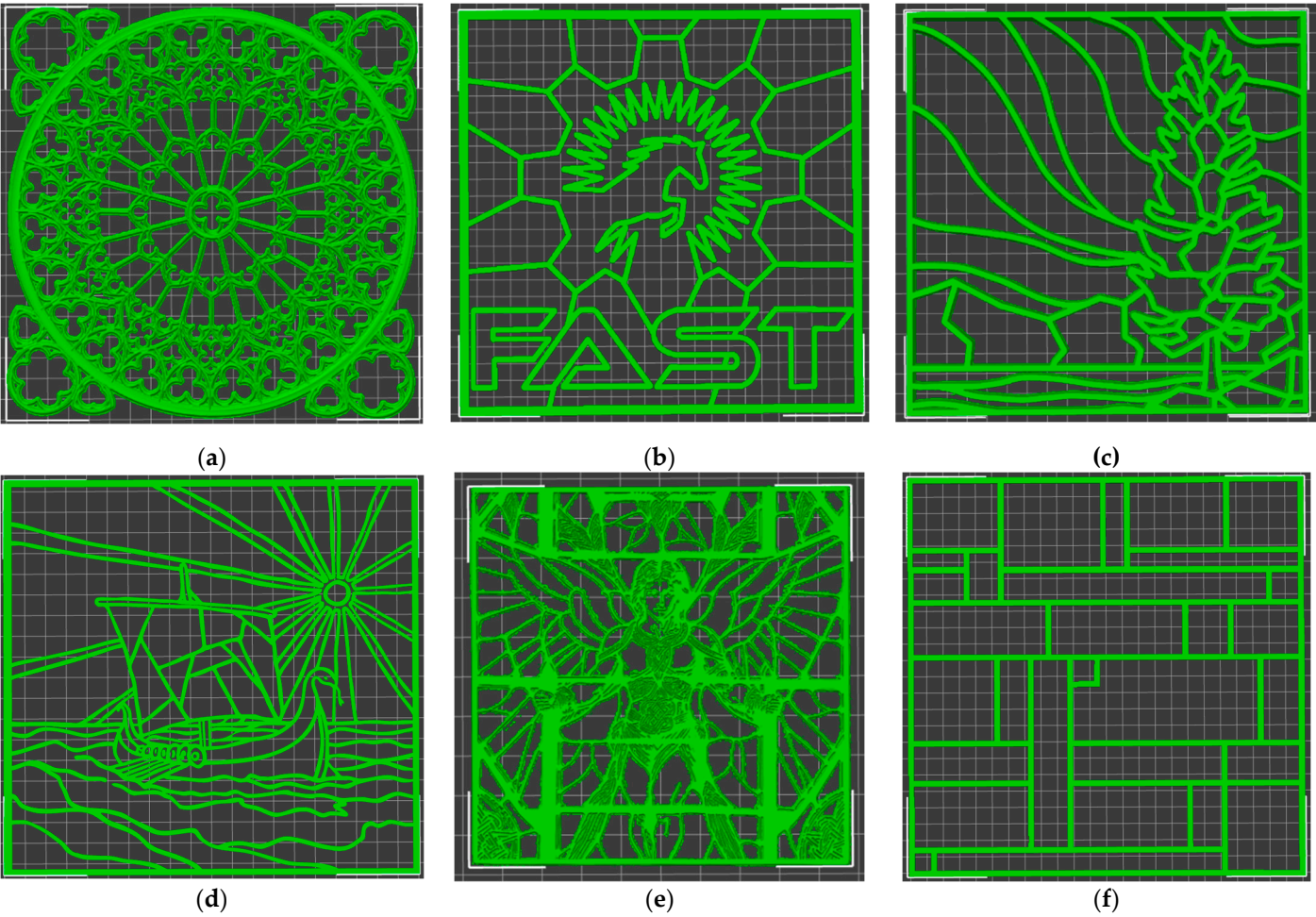


Figure 3. Images of the STL files for the sample designs: (a) Notre Dame Rose Window (SG01); (b) FAST logo (SG02); (c) Northern Lights (SG03); (d) Viking Ship (SG04); (e) Angel (SG05); (f) Geometric calibration pattern (SG06).

2.3. Phases 4 and 5: FFF Additive Manufacturing and Painting

The gcode files were used to fabricate the PC-based 3D design on the PC substrate via FFF 3D printing. An open-source large-format Modix BIG-Meter FFF 3D printer (Modix GmbH, Koblenz, Germany) [55,56] was used to 3D print the customized stained-glass designs with black PC filament (CC3D, Hangzhou Zhuopu New Materials Technology Co., LTD, China) [57]. The six designs were 3D printed on 304.8 × 304.8 mm PC sheets (Plastic World, North York, Canada) used as substrates, corresponding to an area of 92,900 mm² (one square foot) [58]. The PC sheets were secured to the 3D printing bed with duct tape, and the starting z-height was set at the thickness of the sheet, which means 3 mm. The auto-bed detection thus started the 3D print at just the surface of the PC sheet. In this way, while printing, the 3D printing hotend melted some of the top surface of the sheet, providing a complete bond between the 3D printed PC filament and the PC substrate.

The 3D printed designs were then post-processed to remove any residue material from the process, e.g., stringing, and colored with a 1:1 ratio of paint to water using acrylic paint (Castle Arts Supplies Ltd, Newcastle, UK, and Shuttle Art, California, US). Acrylic paints were selected for their well-known good UV stability, matching the intended application. The painted stained glass parts were then dried at room temperature for 1 hour before further characterization analyses.

2.4. Optical Spectrum Characterization and Transmission Calculation

The stained glass sample design of the geometric validation pattern (SG06) was used for the optical characterization to validate the presented methodology. This sample was used to perform optical spectrum measurements by means of a custom optical setup (Figure 4) with fiber optic cables coupling: (i) an Ocean Insight HL-2000-FHSA Halogen Light source (Figure 4, left), which was used to illuminate samples held in (ii) an Ocean Insight Square One Cuvette holder (Figure 4, center), and (iii) an Ocean Insight FLAME Spectrometer (Ocean Optics, Figure 4, right) to measure the transmitted light.

The optical transmission of the colored PC sheets was measured from 200 nm to 1040 nm to determine the optical transmission of the acrylic paints. Data were then plotted from 400 nm to 850 nm to focus the analysis on the visible spectrum region and the first portion of the near-infrared spectrum, according to the application studied in this work. To set up the spectrometer, a black out and full light calibration spectra were run. The transparent PC squares were then placed on the light side flush with the side of the cuvette hole to obtain the spectral transmission of the 3 mm thick PC, which was 87.3. This procedure was repeated for the painted PC squares of each of the six colors used for validation, i.e., red, yellow, light green, dark green, light blue, and dark blue. Ocean View software was used to control the spectrometer and process measurements (Ocean Optics) [59].

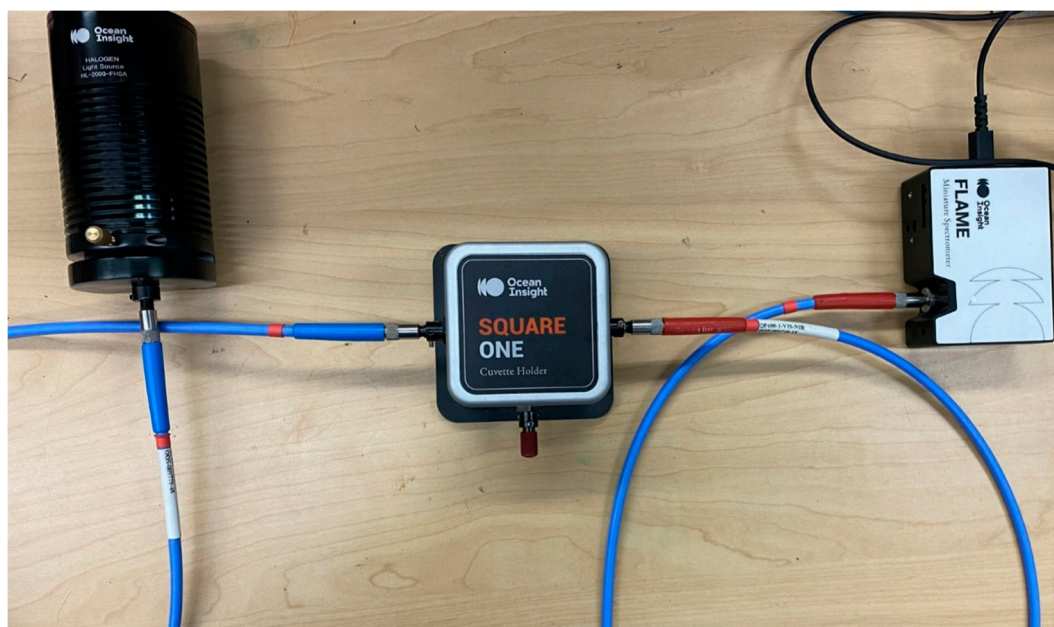


Figure 4. Optical spectra characterization setup comprising a light source (on the left), cuvette holder (center), and spectrometer (on the right).

The total optical transmission of the painted stained glass sample design (SG06) with different colors was calculated using ImageJ. The optical transmission for any multi-colored window can be given according to Equation 1:

$$T = \frac{(\sum_{n=1}^C t_n a_n)}{\sum_{n=1}^C a_n}, \quad (1)$$

Where t is the transmission of color n , a is the over area n , and C is the total number of colors. To test the ability of the image analysis software ImageJ to quantify the area of the colored regions in a PC-based stained glass image, the geometric calibration pattern (SG06) shown in Figure 2f is used and colored according to the scheme of Figure 5. In detail, Figure 5a shows the color codes, where 1 is red, 2 is yellow, 3 is light green, 4 is dark green, 5 is light blue, and 6 is dark blue, whereas Figure 5b shows the known area in mm^2 for the each of the colored regions.

For the example of Figure 6, the total transmission is thus given from Equation 2:

$$T = \frac{(t_1 a_1 + t_2 a_2 + t_3 a_3 + t_4 a_4 + t_5 a_5 + t_6 a_6)}{(a_1 + a_2 + a_3 + a_4 + a_5 + a_6 + a_p)} \quad (2)$$

Where the six colors used in SG06 are taken into account and a_p is the area of the black 3D-printed PC lines with an optical transmission of 0%. The experimental data are available in the OSF repository [46].

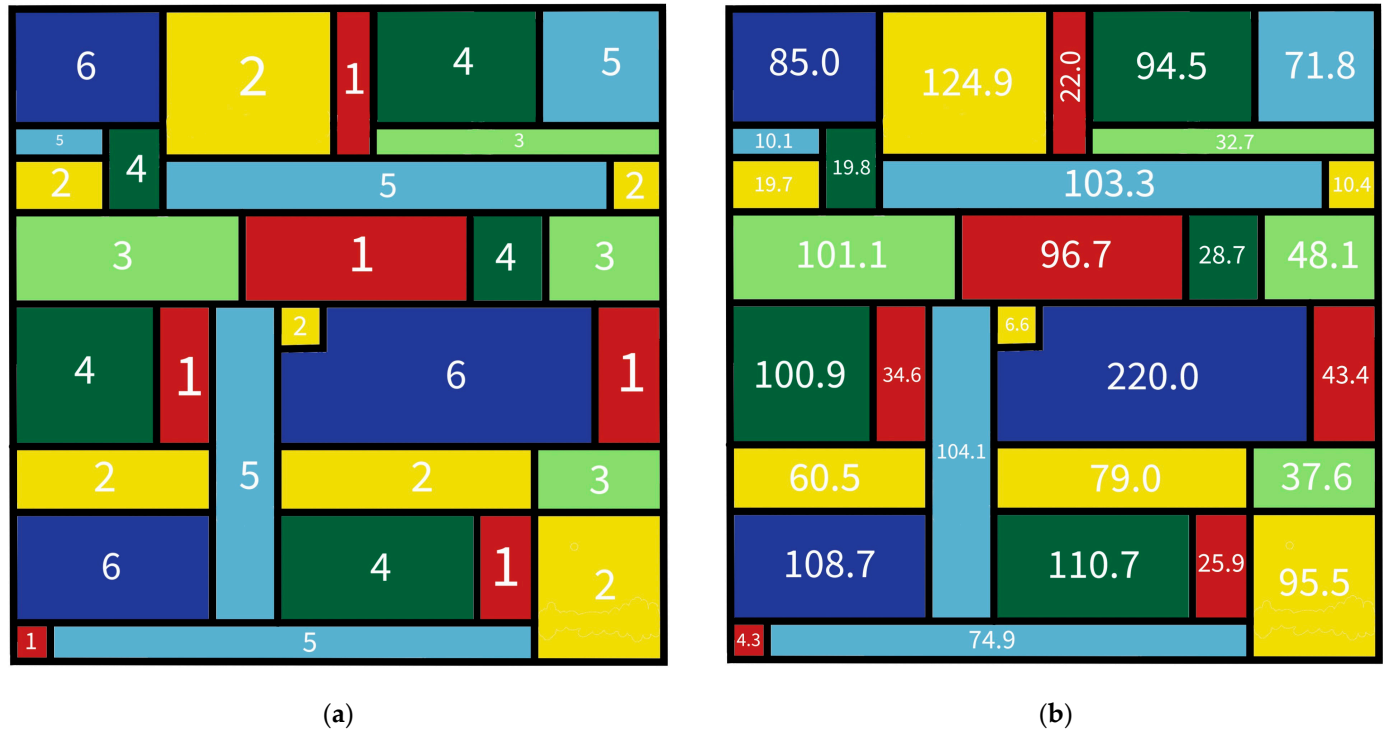


Figure 5. Coloring scheme of the geometric calibration pattern design (SG06), showing the (a) color-coded numbers and (b) area of each colored section in mm².

2.5. Preliminary Economic Analysis

A preliminary economic analysis of the 3D printed PC stained glass alternatives was performed on the six sample designs to validate their suitability in real-world distributed manufacturing contexts, e.g., developing countries. The analysis was performed according to Wittbrodt et al. [60], including materials and fabrication costs from electricity. The 3D printing times and costs were quantified considering the fabrication of the geometric design as an example of a possible design, starting from the nominal times and weights reported from the slicing in PrusaSlicer. The nominal weight was calculated assuming an average density of 1.2 g/cm³ for the 3D printed PC feedstock, whereas the cost was US\$ 19.32/kg of filament [57]. According to the producer, an average power consumption of 1650 W was considered for fabricating the 3D printed PC path on the selected large-format Modix 3D printer [61], i.e., 1370 W for the heated bed and 280 W for the 3D printer electronics, with an average electricity cost of US\$ 0.088, extracted from the mid-peak price period datasheet of the Ontario Energy Board [62]. The cost of PC sheets was US\$ 4.20/m² for batches lower than 100 m² [63], whereas a low-cost acrylic paint set of the selected brand cost about US\$ 22. The calculations are available in the OSF repository [46].

3. Results and Discussion

3.1. FFF Additive Manufacturing of the Sample Designs

Figure 6 shows the 3D printed PC-based stained glass designs obtained from the FFF 3D printing process (Section 2.3). The different sample designs (Table 1) were successfully fabricated by using the

3D printing parameters reported in Table 3. The overall quality of the 3D printed paths is satisfactory for all the samples. No warping and local delamination were detected during the 3D printing and cooling times. This fact indicates the good quality of the bonding between the PC substrate and the 3D printed PC paths thanks to the bonding method described in Section 2.3, i.e., partial melting of the substrate thanks to the partial contact of the hotend 3D printing toolpath and the substrate (Figure 6a). On the one hand, this choice helped increase the durability of the connection between the 3D-printed part and the substrate. On the other hand, it might decrease the accuracy of the 3D printed patterns by increasing the width of the first layer lines, also known as the “elephant foot” effect, e.g., SG02 (Figures 2b, 3b, and 6b). This feature can be easily adjusted by modifying the original line width of the 2D image and 3D mesh model, especially for custom vector designs made by the user.

The online-retrieved designs (SG01 and SG02) showed different results in terms of quality, also connected with their original image format, i.e., raster (SG01) and vector (SG02). The former design (Figure 6a) has intricate patterns, less homogeneous line thicknesses, and uses different widths to reproduce complex details, e.g., the trefoil and quatrefoil shapes in the middle, requiring different retractions and toolhead non-printing travels to be achieved, increasing the stringing effect and the overall 3D printing times. The latter (Figure 6b), being a vector logo file, has less intricate patterns made of similar thicknesses, which can be easily fabricated with fewer retractions and toolhead non-printing travels. The custom designs (SG03 and SG04) showed the highest accuracy and 3D printing quality thanks to the use of lines with consistent widths during the drawing phase, resulting in uniform widths of the 3D printed paths, as visible in Figures 6c and 6d. The AI-generated design (SG05) showed the same issues as SG01 in terms of the width of the 3D printed paths, especially visible from the solid black PC areas of the last top layer (Figure 6e). This result is in line with the original format of the 2D image, i.e., raster, and the different formal language of the picture, which has big black drawing portions and very small intricate white details not suitable for the selected nozzle diameter of 0.8 mm (Figure 2e). Finally, the geometric validation image (SG06) reached accuracy levels comparable to the custom designs, in line with the homogeneous line width used for its realization.

These qualitative results show the feasibility of 3D printing design patterns with different shape and geometry complexity. They also highlight the need for optimized 3D path designs to achieve optimal results, i.e., reduced stringing and increased shape and line width accuracy, requiring approaches toward DfAM. As suggested by works on tunable 2D paths for 3D printing [42,43], the conversion of the 2D designs into 3D printing paths can be optimized to reduce the creation of shape defects from the approximation due to the nozzle diameter and movement path generation, e.g., controlling their width and the distance between the lines. The 3D printing quality of the patterns can also be improved by using different nozzle diameters to fabricate different line widths of the 2D image, especially when using a multi-toolhead or dual-extruder 3D printer as the Modix. For instance, the 3D mesh model can be divided into two separate portions, each to be assigned to a specific hotend mounting different nozzle sizes, e.g., 0.8 mm for the main paths and 0.4 mm for fine details. This choice can also increase the aesthetic possibilities that can be achieved by 3D printing stained glass alternatives, increasing the potential uses by applying DfAM principles.



Figure 6. 3D printed stained glass sample designs with black PC filaments on clear PC sheets substrates of (a) Notre Dame rose window (SG01) during the 3D printing process and post-printing of: (b) FAST logo (SG02); (c) Northern Lights (SG03); (d) Viking Ship (SG04); (e) Angel (SG05); and (f) Geometric calibration pattern (SG06).

3.2. Aesthetic Production of Designs

3.2.1. Online-Retrieved Designs

Figure 7a shows the painted stained glass alternative of the Rose Window on the Notre Dame Cathedral design (SG01). As can be seen in the image, the non-uniform effect of using the watered-down acrylic paint creates an authentic-looking old-colored glass effect. As the design has a high fraction of dark blue and red, the overall transparency of the window is also high. This fact is because the dark blue and red paints have no white in their solutions, making the colors less opaque. Figure 7b shows the finalized image of the FAST lab logo (SG02), which was painted in purple tones according to the Western University color palette. This first approach demonstrated the feasibility of using already available 2D images as 3D printing patterns for stained glass alternatives.

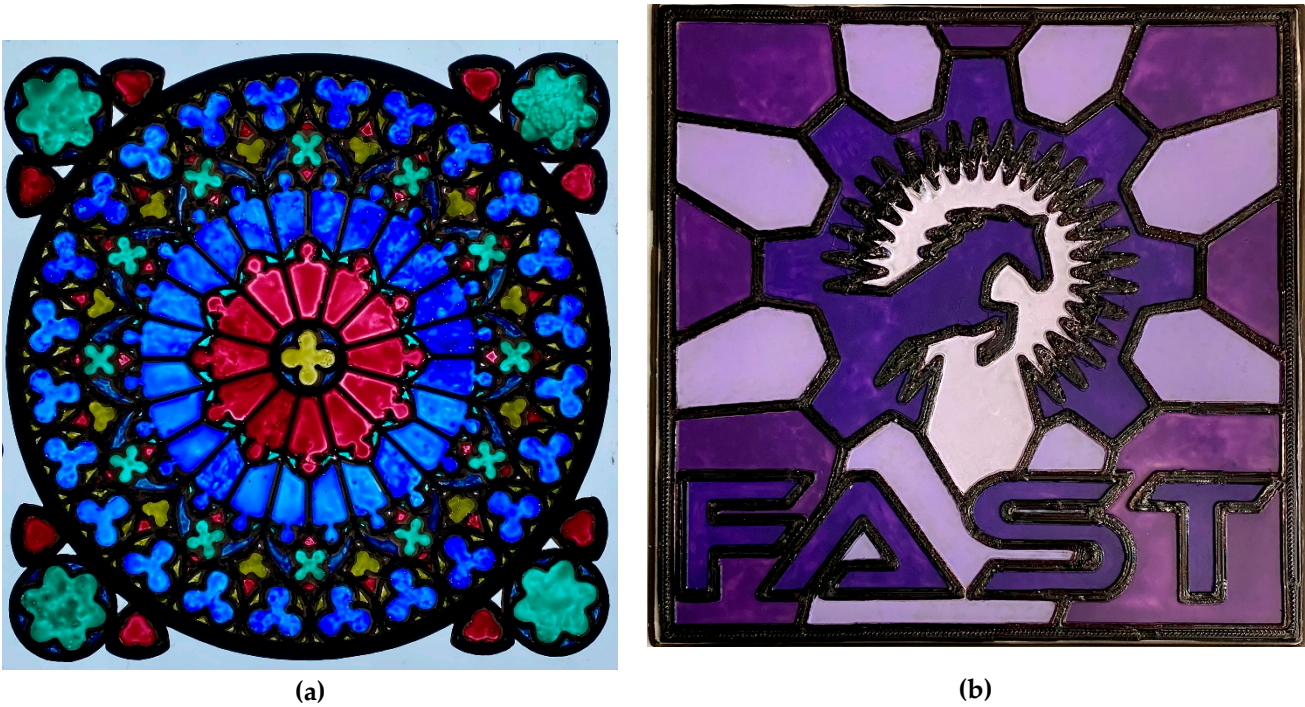


Figure 7. 3D printed stained glass sample design of the online retrieved designs after acrylic painting: (a) Notre Dame rose window (SG01); and (b) FAST Logo (SG02).

3.2.2. Custom Designs: Digital-Drawn and Hand-Drawn Images

Figure 8 shows the two hand-drawn stained glass sample designs made as custom patterns after painting. Figure 8a shows the digitally hand-drawn painting of the Northern lights, while Figure 8b shows the results from the digitally acquired sketch of the Viking ship, photographed and post-processed to ensure consistent line widths. This approach showed the ability to customize stained glass alternatives according to specific user's designs, increasing the range of potential options for 3D-printed stained glass.



Figure 8. 3D printed stained glass sample designs of the custom designs after acrylic painting: (a) Northern Lights (SG03, digitally hand-drawn image); and (b) Viking Ship (SG04, digitally-acquired hand-drawn image).

3.2.3. AI-Generated Design and Geometric Validation Image

Figure 9a shows the AI-generated sample design after painting (SG05), showing a further potential way to customize 3D-printed stained glass alternatives. This solution can be useful for users: (i) unable to find already available images on the Internet matching their needs; (ii) without adequate artistic, technical, or design skills; or (iii) without enough time to design their own design patterns. Open-source AI generation tools like Stable Diffusion can also be used to make new designs using appropriate prompts. Lastly, basic geometric patterns (SG06, Figure 9b) can also be customized and done using vector software without significant sketching or artistic drawing skills.

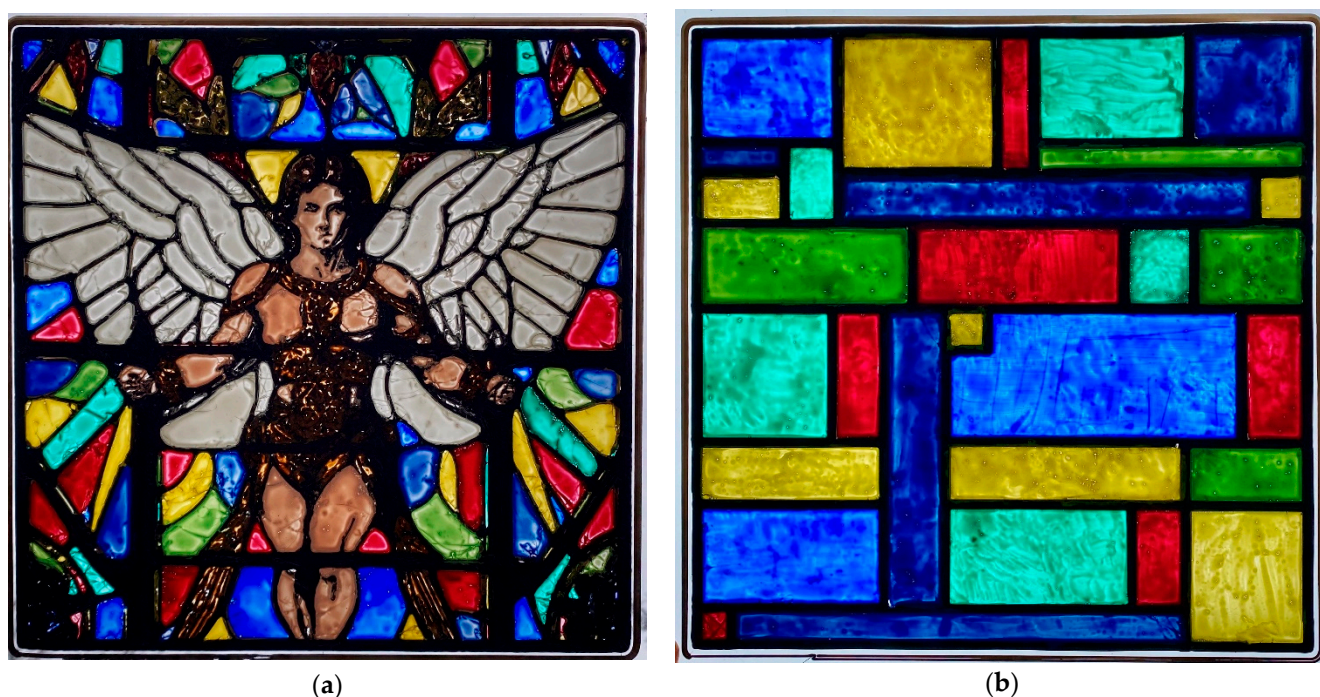


Figure 9. 3D printed stained glass sample designs after acrylic painting of the: (a) AI-generated design (Angel, SG05); and (b) Geometric validation image (SG06) with sunlight back illumination.

3.3. Optical Transmission Validation

The optical characterization was performed on the painted geometric validation pattern (SG06) to validate the methodology presented in this work. The optical transmission as a function of wavelength for the six color hues selected for the validation study is shown in Figure 10. The dark blue hue had the highest light transmission peaks in the visible region (4000-750 nm), whereas the lowest transmission values were observed in the light green and light blue hues. This fact is because of substantial fractions of white pigment in the formulations of light color hues, e.g., titanium dioxide, which can scatter or absorb the light transmission, resulting in more opaque painted colors despite their light tones and the clear substrate [64]. Some hues exhibited sharp drops in the transmission in the 500-600 nm and 700-800 nm regions, i.e., dark blue, dark green, and red, which can be due to the specific pigment spectral behavior from their formulation. Light colors show smoother transmittance curves without significant peak drops, i.e., yellow and light blue, or with a flat profile, such as for the light green hue. Furthermore, the presence of UV-blockers in the acrylic formulations to improve the UV resistance of the paints can justify the low light transmittance values close to 400 nm, then recovered in the visible region. This behavior is also visible in the clear PC substrate, known for its UV resistance. Although the acrylic-painted PC stained glass uses different coloring ways than traditional techniques, these results can be used for a preliminary assessment of the painting method, helping optimize the painting procedure according to the desired color and light perception, e.g., water mixing ratio, number of painting layers, or hue mixing.

The finalized geometric design used for validation (Figure 9b) was then used to calculate the total optical transmission of a complete sample design painted stained glass, which also includes the 3D printed PC black design patterns. The areas of the colored regions were all calculated from the digital design (SG06) and verified with calipers to test the accuracy of the ImageJ analysis. As shown in Table 4, the values provided by ImageJ are within rounding error for all regions, e.g., 0.1 mm². ImageJ can, therefore, provide good accuracy for evaluating area fractions on more complicated patterns. It can then be used to evaluate the total optical transmission of painted 3D-printed stained glass using the general equation for optical transmission (Equation 1), further supporting the fully open-source toolchain. The measurements were repeated three times for each pigment to ensure the repeatability of the procedure, but no significant differences or variations were observed. According to Equation 2, the total transmittance of the geometric design (SG06) shown in Figure 9b is 6.46%, strongly influenced by the 3D-printed black PC patterns (came alternatives). As for the previous optical characterization, this assessment can be used to design geometry patterns and paint color combinations to achieve specific requirements, e.g., daylight-transmitting surfaces or smooth-colored light diffusion. This approach allows for flexibility in the design of the stained glass alternatives by tuning the proportions of 3D printed black frames, clear PC, and painted surfaces.

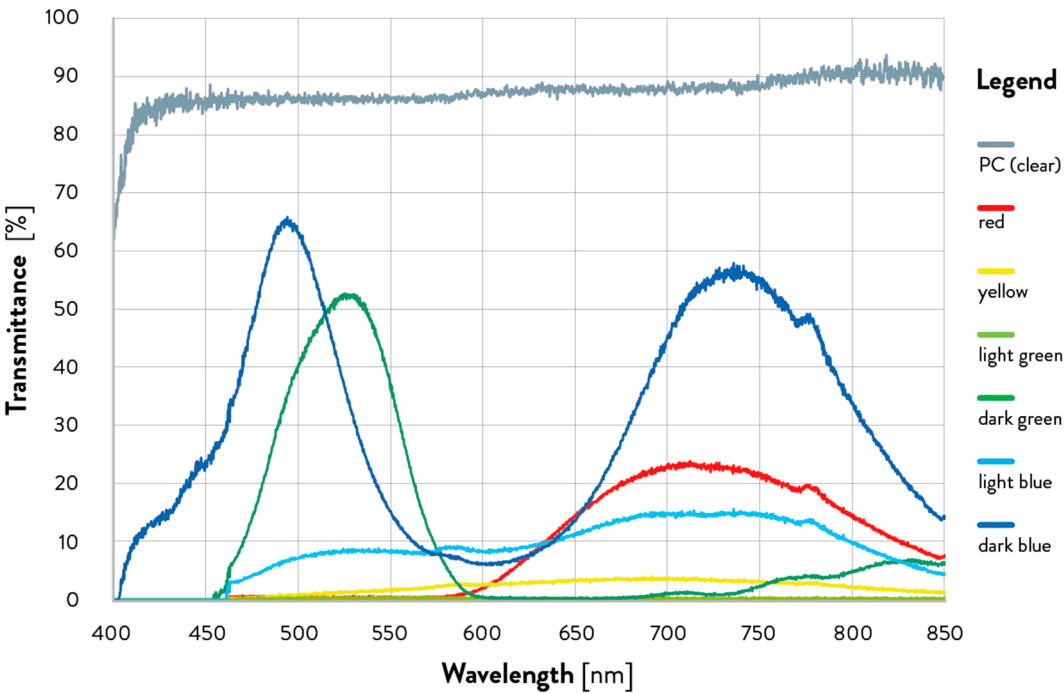


Figure 10. The spectral transmittance as a function of wavelength of the clear PC substrate and of the PC substrate areas with the six sample acrylic paint hues.

Table 4. Optical transmission of the PC substrate areas with the six sample acrylic paints used in the geometric validation design, along with the calculated areas.

N. Color	Color	Transmission (%)	Area in the Geometric Validation Design (mm ²)
1	Red	7.5	226.9
2	Yellow	1.7	396.4
3	Light Green	0.1	219.2
4	Dark Green	7.6	354.7
5	Light Blue	6.9	364.3
6	Dark blue	21.3	413.6

3.4. Economic Analysis

A preliminary economic analysis of the stained glass PC sample designs was performed to validate its suitability in real-world distributed manufacturing contexts, such as developing countries, including the base material and energy consumption costs. The 3D printing weights, times, and costs were quantified for the six sample designs, starting from the nominal times reported from the slicing in PrusaSlicer, as shown in Table 5. The different design patterns required less than 1 h to be fabricated, whereas the geometric design (SG06) took about 20 minutes of 3D printing time to fabricate. The primary cost was the 3D printing PC filament, with average weights of 20-30 g and costs of 0.40-0.60 US\$ in most cases. For instance, the geometric validation sample (SG06) used 21 g of PC filament, which costs US\$ 19.32/kg [57], so the filament cost was about US\$ 0.41. Energy costs represent a minimal percentage of the overall costs to fabricate the 3D-printed glass sample designs. Previous work on distributed manufacturing using open-source 3D printers has already shown that the electrical costs of 3D printing are greatly exceeded by the cost of filament [27]. The analysis further confirmed it, reaching average values of US\$ ~0.10 despite the significant impact of the heating bed on the energy consumption of large-format 3D printers [61,65].

The secondary cost is the PC sheet. PC sheets in relatively small batches (>100 m²) can be obtained for US\$4.20/m² [63], which makes the PC experimental sheet cost about US\$ 0.39. The paint was estimated to cost only a few pennies for each sample, hence negligible in this analysis. Thus, the total material cost per square foot is around US\$ 11-12/m² (US\$ ~1/ft²). For comparison, the cost of a standard double pane window is US\$ 50/m² (US\$ 4.64/ft²) [66], and stained glass, as noted earlier, costs US\$ 6,372/m² (US\$ 592/ft²). Thus, this approach reduces the material and energy costs for stained glass as an alternative by more than a factor of ~50, with significant differences between parts with optimized 3D printed paths, e.g., SG04, and designs created without the same optimization, such as the AI-generated sample (SG05).

Table 5. Economic analysis of the six different 3D printed PC stained glass sample designs.

Sample	3D printed path				PC substrate	Total cost (US\$)
	Nominal weight (g)	Nominal time (min)	Material cost (US\$)	Energy cost (US\$)	Sheet cost (US\$)	
SG01	30.2	57	0.58	0.14	0.39	1.11
SG02	29.8	44	0.58	0.11	0.39	1.07
SG03	33.2	32	0.64	0.08	0.39	1.11
SG04	30.4	32	0.59	0.08	0.39	1.06
SG05	39.0	74	0.75	0.18	0.39	1.32
SG06	21.0	20	0.41	0.05	0.39	0.85

3.5. Potential of 3D Printed Stained Glass Alternatives Fabricated Through Open-Source Approaches

The results of this study demonstrated a new open-design approach to obtaining stained glass alternatives using a fully open-source toolchain made up of open-source software and open hardware-based additive manufacturing. This methodology can be applied to different 2D images and 3D mesh models, generating customized stained-glass designs from online-retrieved files found on the internet, as well as novel custom design patterns, either developed natively in digital media or digitally acquired from hand-drawn on paper. In addition, open-source AI image generators can be used to generate stained-glass designs. These approaches, as well as the whole methodology, provide an accessible and flexible way to add or replace stained glass windows with a (i) thermally superior, (ii) low-cost, and (iii) customizable PC-based stained glass alternative available to a broader range of users and customers.

This application of 3D printing is in line with other work that has applied AM technologies for buildings and cultural heritage [67]. Current AM applications include the conservation and restoration of architectural structures, artworks, and cultural artifacts, e.g., columns or sculptures

[68,69], as well as the design and development of entirely new artifacts, products, and artworks [70]. Among these, first attempts in partially or fully 3D print stained glass-like parts have been emerging recently, ranging from small Do-It-Yourself samples [71] and colored epoxy casting into 3D printed frames [72] to commercial 3D printed clear resin windows mounted into 3D printed frames after painting [73]. To this end, the open design methodology presented in this work can support the real implementation of stained glass alternatives in different contexts. Specifically, broken stained glass windows that need to be replaced could be replicated in PC and inserted into the window opening directly or as part of a sandwich with a conventional clear window. In addition, new stained glass windows could be designed to be used in cultural buildings and public spaces or as part of new products or hybrid craft practices [14]. Existing historical designs can also be replicated in different geographical contexts, either for replicative or educational purposes, taking advantage of the distributed nature of AM technologies. Lastly, using secondary raw materials from scraps and byproducts can pave the way to distributed 3D-printed stained glass alternatives from locally recycled feedstocks, following the principles of distributed recycling for additive manufacturing (DRAM) [39,74]. These materials are currently used to fabricate several products with large-format 3D printers, including architectural elements and artistic artifacts [75]. Stained glass alternatives can, therefore, further enlarge the available applications in real-world scenarios, e.g., specific geographical or low-resource settings.

The rectilinear geometric shape-related analysis successfully demonstrated that open-source ImageJ software can be effectively utilized to quantify the areas of stained glass for quantitative evaluations. These areas can then be coupled with measured optical spectral transmission measurements to gain complete transmission values of full stained glass window alternatives with more complex shapes and designs, as shown in the previous section. This achievement can help design custom patterns according to the desired needs, e.g., specific transmission and diffusion of the window, changes in the ratios between the black frames and the painted clear PC, or adjustments in the painting mixing and procedures. The total optical transmission values found show substantial promise for PC-based stained glass windows to reduce solar heat gain coefficients for windows everywhere, but most importantly in areas with substantial cooling loads.

3.6. Limitations and Future Work

This research presents some limitations to be further studied in future work. For instance, a quantitative assessment of the bonding between the PC substrate and 3D printed paths was not included in the experimental work. Future research can, therefore, study the adhesion of the 3D printed parts onto the substrate, e.g., through pull-off tests. Similarly, the dimensional accuracy of the 3D printed paths should be investigated through quantitative measurements, e.g., comparing the nominal and actual line widths through imaging with ImageJ. This analysis can also be matched with the optimization of the design and fabrication of the 3D printing paths to increase the shape accuracy of complex geometrical shapes while decreasing retractions, travel movements, and 3D printing times, according to DfAM principles. Another limitation of this study was the exclusion of labor for the economic analysis, which only attempted to quantify material and energy consumption costs. The results of the economic analysis showed that PC-based stained glass alternatives have the potential to cut that price by a factor of 50. Labor costs would include the labor to set up the 3D printing process (minor), as well as to color the PC, which could be substantial depending on the labor costs. Thus, the labor costs may be more expensive than the equipment. The energy efficiency of the proposed stained glass alternative should also be evaluated to validate its use in different geographical and socio-economic contexts, and future work is needed to quantify the potential energy savings for such PC-based stained glass windows applications.

Additional work can be done to further spread the potential use of the proposed stained glass alternatives. For instance, it is possible to use a multi-toolhead or multi-extruder 3D printer to fully 3D print stained glass designs with translucent filaments of different colors [76], but this approach was not used here because of the current unavailability of translucent PC filaments. Thus, substantial

future work is needed to develop such filaments using recycled PC and open-source waste plastic extruders, e.g., recyclebots [74,77]. Different nozzle diameters could also be matched in a single design pattern by means of multi-toolhead or dual-extruder 3D printers, assigning specific nozzle sizes to geometrical features with different line widths and intricate shapes, optimizing the fabrication process and enlarging the design flexibility. Another approach could be the Hueforge filament painting approach of 3D printing very thin colored filaments that are effectively semi-transparent to make images [78]. In the future, using a multi-toolhead or multi-material 3-D printer to deposit different filament colors on top of UV-stabilized PC sheets is an area to be explored for complete stained glass replacements. There have been efforts to convert conventional images to stained glass-like images using a combination of image warping, segmentation, querying, colorization, and texture synthesis [79]. This approach was used here with Stable Diffusion, as stained glass images have also gained popularity with the AI-based art community [80]. Thus, if combined, future work could develop a completely integrated software package for file conversion. This option could allow users to convert a 2D image in a single step to a 3D model and color map file to be fully manufactured on an open-source 3D printer, including coloring, relying on a fully open-source toolchain and methodology.

4. Conclusions

This work explored the use of open-source AM technologies to fabricate PC-based stained glass alternatives for the building and heritage sectors, providing a way for customizable, low-cost, and thermally superior options compared to conventional products. It presented a new DfAM methodology for 3D printable stained glass alternatives based on open design principles, i.e., using a fully open-source toolchain for all the steps. Different design patterns were created through three approaches, i.e., from online-retrieved 2D images or 3D models, custom digitalized or digital drawings, and AI-generated 2D images. The six sample designs were successfully fabricated using PC sheets as substrates for 3D-printed custom geometries made in PC, which were then painted with acrylic colors. The methodology was then validated through optical characterization with open-source software and a preliminary economic analysis, highlighting the potential use of these alternatives in specific geographical and low-resource settings.

According to the results, different geometries can be fabricated with this approach starting from different sources and formats of the 2D images, e.g., raster or vector files. The custom designs and the vector image sources showed the best results in terms of 3D printing quality and accuracy of the intended shapes, allowing for the optimization of the drawing lines and resulting in optimized 3D printing toolpath generation, such as limited retractions and stringing from travel movements. Further optimization of the 3D printing paths can increase pattern fidelity and design flexibility, especially using multi-nozzle and toolhead 3D printers. Optical spectrum characterization of the painted, stained glass showed different transmittance behaviors due to the acrylic painting hue, whereas the total optical transmission could be estimated based on the specific geometry pattern and the distribution of the different colored and 3D printed areas. This open-source evaluation can be used to customize stained glass alternatives according to the desired light transmission and heat gain behaviors by tuning the 3D printed pattern geometry design and the painting process. Finally, the economic analysis shows substantial cost reduction when using large-format AM technologies and PC as the main material, i.e., up to 50 times less expensive than traditional stained glass.

The proposed methodology shows potential for distributed and accessible applications in the building and heritage sectors, especially for the repair and replication of existing conventional stained glass and the design of new customizable products. Despite the need for further work, initial results show potential application in climate environments to reduce solar heat gain coefficients and manufacturing costs while allowing for design flexibility and aesthetic customization. Future research should (i) deepen the characterization of the fabricated parts, e.g., the dimensional accuracy and bonding of the 3D printed path; (ii) explore multi-extruder and toolhead systems for automated coloring and intricated frame details; (iii) optimize the conversion of the 2D images into 3D printing

paths; and (iv) quantify the energy saving of the proposed stained glass alternatives. Overall, the open design methodology proposed in this work offers an accessible way to foster low-cost, customizable, and energy-efficient architectural and design applications for the building and heritage sectors in broader geographical and socio-economic contexts.

Author Contributions: Conceptualization, E.B.P. and J.M.P.; methodology, E.B.P., J.M.P, A.R.; Software, E.B.P., J.M.P., A.R.; validation, E.B.P. and A.R.; formal analysis, E.B.P. and A.R.; investigation, E.B.P.; resources, J.M.P.; data curation, E.B.P., J.M.P, A.R.; writing—original draft preparation, E.B.P., J.M.P, A.R.; writing—review and editing, E.B.P., J.M.P, A.R.; visualization, E.B.P. and A.R.; supervision, J.M.P. and A.R.; project administration, J.M.P. and A.R.; funding acquisition, J.M.P. and A.R. All authors have read and agreed to the published version of the manuscript.

Funding: Funding for this work was provided by the Canada Foundation for Innovation, the Ontario Research Fund-Research Infrastructure program, the Natural Sciences and Engineering Research Council of Canada, and the Thompson Endowment.

Institutional Review Board Statement: Not applicable.

Informed Consent Statement: Not applicable.

Data Availability Statement: Data is available at <https://osf.io/wq5pf/>.

Acknowledgments: The authors would like to thank J. Givans for technical support.

Conflicts of Interest: The authors declare no conflicts of interest.

References

1. Rosewell, R. Stained Glass; Bloomsbury Publishing, 2012; ISBN 978-1-78200-150-8.
2. Hunault, M.O.J.Y.; Bauchau, F.; Boulanger, K.; Hérold, M.; Calas, G.; Lemasson, Q.; Pichon, L.; Pacheco, C.; Loisel, C. Thirteenth-Century Stained Glass Windows of the Sainte-Chapelle in Paris: An Insight into Medieval Glazing Work Practices. *Journal of Archaeological Science: Reports* 2021, 35, 102753, doi:10.1016/j.jasrep.2020.102753.
3. Varieties of Stained Glass Available online: <https://stainedglass.org/learning-resources/varieties-stained-glass> (accessed on 20 May 2025).
4. Parker, J.M.; Martlew, D. Stained Glass Windows. In *Encyclopedia of Glass Science, Technology, History, and Culture*; John Wiley & Sons, Ltd, 2021; pp. 1341–1359 ISBN 978-1-118-80101-7.
5. Finucane, M.A.; Black, I. CO₂ Laser Cutting of Stained Glass. *Int J Adv Manuf Technol* 1996, 12, 47–59, doi:10.1007/BF01178961.
6. Rehren, Th.; Freestone, I.C. Ancient Glass: From Kaleidoscope to Crystal Ball. *Journal of Archaeological Science* 2015, 56, 233–241, doi:10.1016/j.jas.2015.02.021.
7. Shields, D. Design in Stained Glass. *Studies: An Irish Quarterly Review* 1952, 41, 209–218.
8. Yuan, M.; Bonet, J.; Cotte, M.; Schibille, N.; Gratuze, B.; Pradell, T. The Role of Sulphur in the Early Production of Copper Red Stained Glass. *Ceramics International* 2023, 49, 18602–18613, doi:10.1016/j.ceramint.2023.02.236.
9. Pradell, T.; Molina, G.; Murcia, S.; Ibáñez, R.; Liu, C.; Molera, J.; Shortland, A.J. Materials, Techniques, and Conservation of Historic Stained Glass “Grisailles.” *International Journal of Applied Glass Science* 2016, 7, 41–58, doi:10.1111/ijag.12125.
10. Verney-Carron, A.; Sessegolo, L.; Chabas, A.; Lombardo, T.; Rossano, S.; Perez, A.; Valbi, V.; Boutillez, C.; Muller, C.; Vaulot, C.; et al. Alteration of Medieval Stained Glass Windows in Atmospheric Medium: Review and Simplified Alteration Model. *npj Mater Degrad* 2023, 7, 1–24, doi:10.1038/s41529-023-00367-0.
11. Vilarigues, M.; Redol, P.; Machado, A.; Rodrigues, P.A.; Alves, L.C.; da Silva, R.C. Corrosion of 15th and Early 16th Century Stained Glass from the Monastery of Batalha Studied with External Ion Beam. *Materials Characterization* 2011, 62, 211–217, doi:10.1016/j.matchar.2010.12.001.

12. M. Corrêa Pinto, A.; Macedo, M.F.; G. Vilarigues, M. The Conservation of Stained-Glass Windows in Latin America: A Literature Overview. *Journal of Cultural Heritage* 2018, 34, 172–181, doi:10.1016/j.culher.2018.04.019.
13. Murcia-Mascarós, S.; Foglia, P.; Santarelli, M.L.; Roldán, C.; Ibañez, R.; Muñoz, A.; Muñoz, P. A New Cleaning Method for Historic Stained Glass Windows. *Journal of Cultural Heritage* 2008, 9, e73–e80, doi:10.1016/j.culher.2008.08.008.
14. Gagnon-King, D.; Jones, L.; Nabil, S. Interactive Stained-Glass: Exploring a New Design Space of Traditional Hybrid Crafts for Novel Fabrication Methods. In *Proceedings of the Proceedings of the Seventeenth International Conference on Tangible, Embedded, and Embodied Interaction; Association for Computing Machinery: New York, NY, USA, February 26 2023; pp. 1–15.*
15. Cuce, E.; Riffat, S.B. A State-of-the-Art Review on Innovative Glazing Technologies. *Renewable and Sustainable Energy Reviews* 2015, 41, 695–714, doi:10.1016/j.rser.2014.08.084.
16. Somasundaram, S.; Thangavelu, S.R.; Chong, A. Improving Building Efficiency Using Low-e Coating Based Retrofit Double Glazing with Solar Films. *Applied Thermal Engineering* 2020, 171, 115064, doi:10.1016/j.applthermaleng.2020.115064.
17. Wolf, S.; Trümpler, S.; Wakili, K.G.; Binder, B.; Baumann, E. Protective Glazing: The Conflict Between Energy- Saving and Conservation Requirements.
18. Uher, C. Thermal Conductivity of Metals. In *Thermal Conductivity: Theory, Properties, and Applications; Tritt, T.M., Ed.; Physics of Solids and Liquids; Springer US: Boston, MA, 2004; pp. 21–91 ISBN 978-0-387-26017-4.*
19. Lidelöw, S.; Örn, T.; Luciani, A.; Rizzo, A. Energy-Efficiency Measures for Heritage Buildings: A Literature Review. *Sustainable Cities and Society* 2019, 45, 231–242, doi:10.1016/j.scs.2018.09.029.
20. Learn How Much It Costs to Install Stained Glass. Available online: <https://www.homeadvisor.com/cost/home-design-and-decor/install-stained-glass/> (accessed on 19 November 2023).
21. How Much Does It Cost to Install a Stained Glass Window in 2023? Available online: <https://www.angi.com/articles/how-much-cost-stained-glass-window.htm> (accessed on 19 November 2023).
22. Stained Glass Repair Cost: Can Stained Glass Be Repaired and How Much Does It Cost? - Kompareit.Com Available online: <https://www.kompareit.com/homeandgarden/windows-can-stained-glass-be-repaired.html#:~:text=How%20Much%20Does%20Stained%20Glass%20Repair%20Cost%3F%201,panel%2C%20depending%20on%20size%20and%20condition.%20More%20items> (accessed on 19 November 2023).
23. Frenzel, G. The Restoration of Medieval Stained Glass. *Scientific American* 1985, 252, 126–137.
24. Qurraie, B.S.; Beyhan, F. Investigating the Effect of Stained-Glass Area on Reducing the Cooling Energy of Buildings (Case Study: Ankara). *CRPASE* 2022, 8, 1–11, doi:10.52547/crpase.8.1.2749.
25. Shaik, S.; Maduru, V.R.; Kirankumar, G.; Arıcı, M.; Ghosh, A.; Kontoleon, K.J.; Afzal, A. Space-Age Energy Saving, Carbon Emission Mitigation and Color Rendering Perspective of Architectural Antique Stained Glass Windows. *Energy* 2022, 259, 124898, doi:10.1016/j.energy.2022.124898.
26. Moretti, E.; Zinzi, M.; Belloni, E. Polycarbonate Panels for Buildings: Experimental Investigation of Thermal and Optical Performance. *Energy and Buildings* 2014, 70, 23–35, doi:10.1016/j.enbuild.2013.11.045.
27. Wittbrodt, B.T.; Glover, A.G.; Laureto, J.; Anzalone, G.C.; Oppliger, D.; Irwin, J.L.; Pearce, J.M. Life-Cycle Economic Analysis of Distributed Manufacturing with Open-Source 3-D Printers. *Mechatronics* 2013, 23, 713–726, doi:10.1016/j.mechatronics.2013.06.002.
28. Attaran, M. The Rise of 3-D Printing: The Advantages of Additive Manufacturing over Traditional Manufacturing. *Business Horizons* 2017, 60, 677–688, doi:10.1016/j.bushor.2017.05.011.
29. Romani, A.; Rognoli, V.; Levi, M. Design, Materials, and Extrusion-Based Additive Manufacturing in Circular Economy Contexts: From Waste to New Products. *Sustainability* 2021, 13, 7269, doi:10.3390/su13137269.
30. Obi, M.U.; Pradel, P.; Sinclair, M.; Bibb, R. A Bibliometric Analysis of Research in Design for Additive Manufacturing. *Rapid Prototyping J.* 2022, 28, 967–987, doi:10.1108/RPJ-11-2020-0291.

31. Boisseau, É.; Omhover, J.-F.; Bouchard, C. Open-Design: A State of the Art Review. *Des. Sci.* 2018, 4, e3, doi:10.1017/dsj.2017.25.
32. Sells, E.; Bailard, S.; Smith, Z.; Bowyer, A.; Olliver, V. RepRap: The Replicating Rapid Prototyper: Maximizing Customizability by Breeding the Means of Production. In *Handbook of Research in Mass Customization and Personalization*; World Scientific Publishing Company, 2009; pp. 568–580 ISBN 978-981-4280-25-9.
33. Jones, R.; Haufe, P.; Sells, E.; Iravani, P.; Olliver, V.; Palmer, C.; Bowyer, A. RepRap – the Replicating Rapid Prototyper. *Robotica* 2011, 29, 177–191, doi:10.1017/S026357471000069X.
34. Petersen, E.E.; Pearce, J. Emergence of Home Manufacturing in the Developed World: Return on Investment for Open-Source 3-D Printers. *Technologies* 2017, 5, 7, doi:10.3390/technologies5010007.
35. Pearce, J.; Qian, J.-Y. Economic Impact of DIY Home Manufacturing of Consumer Products with Low-Cost 3D Printing from Free and Open Source Designs. *European Journal of Social Impact and Circular Economy* 2022, 3, 1–24, doi:10.13135/2704-9906/6508.
36. Bahar, A.; Belhabib, S.; Guessasma, S.; Benmahiddine, F.; Hamami, A.E.A.; Belarbi, R. Mechanical and Thermal Properties of 3D Printed Polycarbonate. *Energies* 2022, 15, 3686, doi:10.3390/en15103686.
37. Vidakis, N.; Petousis, M.; Kechagias, J.D. A Comprehensive Investigation of the 3D Printing Parameters' Effects on the Mechanical Response of Polycarbonate in Fused Filament Fabrication. *Prog Addit Manuf* 2022, 7, 713–722, doi:10.1007/s40964-021-00258-3.
38. Vidakis, N.; Petousis, M.; Velidakis, E.; Spiridaki, M.; Kechagias, J.D. Mechanical Performance of Fused Filament Fabricated and 3D-Printed Polycarbonate Polymer and Polycarbonate/Cellulose Nanofiber Nanocomposites. *Fibers* 2021, 9, 74, doi:10.3390/fib9110074.
39. Romani, A.; Levi, M.; Pearce, J.M. Recycled Polycarbonate and Polycarbonate/Acrylonitrile Butadiene Styrene Feedstocks for Circular Economy Product Applications with Fused Granular Fabrication-Based Additive Manufacturing. *Sustainable Materials and Technologies* 2023, 38, e00730, doi:10.1016/j.susmat.2023.e00730.
40. Reich, M.J.; Woern, A.L.; Tanikella, N.G.; Pearce, J.M. Mechanical Properties and Applications of Recycled Polycarbonate Particle Material Extrusion-Based Additive Manufacturing. *Materials* 2019, 12, 1642, doi:10.3390/ma12101642.
41. Yang, J.; He, S.; Lu, L. Binary Image Carving for 3D Printing. *Computer-Aided Design* 2019, 114, 191–201, doi:10.1016/j.cad.2019.05.028.
42. Chen, Z.; Chen, W.; Guo, J.; Cao, J.; Zhang, Y.J. Orientation Field Guided Line Abstraction for 3D Printing. *Computer Aided Geometric Design* 2018, 62, 253–262, doi:10.1016/j.cagd.2018.03.014.
43. Bedel, A.; Coudert-Osmont, Y.; Martínez, J.; Nishat, R.I.; Whitesides, S.; Lefebvre, S. Closed Space-Filling Curves with Controlled Orientation for 3D Printing. *Computer Graphics Forum* 2022, 41, 473–492, doi:10.1111/cgf.14488.
44. Powell, A. Democratizing Production through Open Source Knowledge: From Open Software to Open Hardware. *Media, Culture & Society* 2012, 34, 691–708, doi:10.1177/0163443712449497.
45. Gibb, A. *Building Open Source Hardware: DIY Manufacturing for Hackers and Makers*; Addison-Wesley Professional, 2014; ISBN 978-0-13-337390-5.
46. Bow Pearce, E.; Pearce, J.; Romani, A. 3D Printable Designs for Alternatives to Stained Glass for Energy Efficiency and Economic Savings. 2025.
47. NOTRE DAME | 3D CAD Model Library | GrabCAD Available online: <https://grabcad.com/library/notre-dame-4> (accessed on 16 May 2025).
48. File:FASTlogobw.Png Available online: <https://www.appropedia.org/File:FASTlogobw.png> (accessed on 25 November 2023).
49. GIMP Available online: <https://www.gimp.org/> (accessed on 20 November 2023).
50. Developers, I.W. Inkscape - Draw Freely. | Inkscape Available online: <https://inkscape.org/> (accessed on 16 May 2025).
51. Foundation, K. Krita Available online: <https://krita.org/en/> (accessed on 20 November 2023).
52. AUTOMATIC1111 Stable Diffusion Web UI Available online: <https://github.com/AUTOMATIC1111/stable-diffusion-webui> (accessed on 20 November 2023).

53. ImageJ Available online: <https://imagej.net/ij/> (accessed on 17 May 2025).
54. PrusaSlicer | Original Prusa 3D Printers Directly from Josef Prusa Available online: https://www.prusa3d.com/page/prusaslicer_424/ (accessed on 21 July 2023).
55. BIG-Meter – Modix Large 3D Printers Available online: <https://www.modix3d.com/big-meter/> (accessed on 17 May 2025).
56. Operating Manual for Modix Printers Available online: https://www.appropedia.org/Operating_Manual_for_Modix_printers (accessed on 17 May 2025).
57. Black PC Filament 1.75 Mm 3D Printer Filament 1 KG Spool 2.2LBS Dimensional Accuracy +/- 0.05mm 3D Printing Polycarbonate Material: Amazon.ca: Industrial & Scientific Available online: https://www.amazon.ca/Filament-Dimensional-Accuracy-Printing-Polycarbonate/dp/B075XS6NP/ref=sr_1_5?keywords=polycarbonate+filament+1.75&sr=8-5 (accessed on 19 November 2023).
58. 20 Pack 12 x 12 x .02 Inch Clear Plastic Craft Polycarbonate Sheet Thin Clear Plastic Sheet Flexible Transparent Plastic Sheet for Crafts DIY Projects Document Picture Frames Replacement Window Panes : Amazon.ca: Home Available online: <https://www.amazon.ca/Polycarbonate-Flexible-Transparent-Projects-Replacement/dp/B09XZZG8SH> (accessed on 19 November 2023).
59. Software. Ocean Optics.
60. Wittbrodt, B.T.; Glover, A.G.; Laureto, J.; Anzalone, G.C.; Oppliger, D.; Irwin, J.L.; Pearce, J.M. Life-Cycle Economic Analysis of Distributed Manufacturing Withopen-Source 3-D Printers. *Mechatronics* 2013, 23, 713-726, doi:10.1016/j.mechatronics.2013.06.002.
61. BIG-Meter – Modix Large 3D Printers Available online: <https://www.modix3d.com/big-meter/> (accessed on 5 May 2025).
62. Electricity Rates | Ontario Energy Board Available online: <https://www.oeb.ca/consumer-information-and-protection/electricity-rates> (accessed on 5 November 2024).
63. [Hot Item] Transparent 3mm 4mm 5mm 8mm Solid Polycarbonate Sheets for Greenhouse Available online: <https://yunai888.en.made-in-china.com/product/uwCtIAPjrzWd/China-Transparent-3mm-4mm-5mm-8mm-Solid-Polycarbonate-Sheets-for-Greenhouse.html> (accessed on 17 May 2025).
64. Costanzo, V.; Nocera, F.; Evola, G.; Buratti, C.; Lo Faro, A.; Marletta, L.; Domenighini, P. Optical Characterization of Historical Coloured Stained Glasses in Winter Gardens and Their Modelling in Daylight Availability Simulations. *Solar Energy* 2022, 243, 22–34, doi:10.1016/j.solener.2022.07.043.
65. Elbadawi, M.; Basit, A.W.; Gaisford, S. Energy Consumption and Carbon Footprint of 3D Printing in Pharmaceutical Manufacture. *International Journal of Pharmaceutics* 2023, 639, 122926, doi:10.1016/j.ijpharm.2023.122926.
66. [Hot Item] Tempered Double Pane Glazing Glass Price Available online: <https://jinjingglass.en.made-in-china.com/product/WdqAnZKyLBRG/China-Tempered-Double-Pane-Glazing-Glass-Price.html> (accessed on 17 May 2025).
67. Balletti, C.; Ballarin, M.; Guerra, F. 3D Printing: State of the Art and Future Perspectives. *Journal of Cultural Heritage* 2017, 26, 172–182, doi:10.1016/j.culher.2017.02.010.
68. Bourgeois, I.; Ascensão, Guilherme; Ferreira, Victor; and Rodrigues, H. Methodology for the Application of 3D Technologies for the Conservation and Recovery of Built Heritage Elements. *International Journal of Architectural Heritage* 2024, 0, 1–12, doi:10.1080/15583058.2024.2341327.
69. Garcia-Espinel, J.D.; González, J.M.L.-G.; Torres, M.F. 3D Heritage: Preserving Historical and Cultural Heritage Through Reality Capture and Large-Scale 3D Printing. In *Decoding Cultural Heritage: A Critical Dissection and Taxonomy of Human Creativity through Digital Tools*; Moral-Andrés, F., Merino-Gómez, E., Reviriego, P., Eds.; Springer Nature Switzerland: Cham, 2024; pp. 377–394 ISBN 978-3-031-57675-1.
70. Yu, J. The Application of 3D Printing Technology in Sculpture. In *Proceedings of the The 2020 International Conference on Machine Learning and Big Data Analytics for IoT Security and Privacy*; MacIntyre, J., Zhao, J., Ma, X., Eds.; Springer International Publishing: Cham, 2021; pp. 755–759.
71. KurtH3 How to 3D Print a Stained “Glass” Window Available online: <https://www.instructables.com/How-to-3D-Print-a-Stained-Glass-Window/> (accessed on 5 March 2025).
72. By Faux Stained Glass Effect, With 3D Printing And Epoxy. Hackaday 2021.

73. cp_admin Toronto Based 3D Printing Service Company Creates a Stained Glass Window out of 100% Plastic Available online: <https://customprototypes.ca/blog/toronto-based-3d-printing-service-company-creates-a-stained-glass-window-out-of-10089991592657516849e6744e94e5940d3ea60f047fd6ba2f5bb1206c368e04806-plastic/> (accessed on 5 March 2025).
74. Zhong, S.; Pearce, J.M. Tightening the Loop on the Circular Economy: Coupled Distributed Recycling and Manufacturing with Recyclebot and RepRap 3-D Printing. *Resources, Conservation and Recycling* 2018, 128, 48–58, doi:10.1016/j.resconrec.2017.09.023.
75. Romani, A.; Levi, M. Large-Format Material Extrusion Additive Manufacturing for Circular Economy Practices: A Focus on Product Applications with Materials from Recycled Plastics and Biomass Waste. *Sustainability* 2024, 16, 7966, doi:10.3390/su16187966.
76. Thingiverse.com Stained Glass Orchid by Carbonbased Available online: <https://www.thingiverse.com/thing:3080869> (accessed on 20 November 2023).
77. Woern, A.L.; McCaslin, J.R.; Pringle, A.M.; Pearce, J.M. RepRapable Recyclebot: Open Source 3-D Printable Extruder for Converting Plastic to 3-D Printing Filament. *HardwareX* 2018, 4, e00026, doi:10.1016/j.ohx.2018.e00026.
78. Home of HueForge Available online: <https://shop.thehueforge.com/> (accessed on 17 May 2025).
79. Brooks, S. Image-Based Stained Glass. *IEEE Transactions on Visualization and Computer Graphics* 2006, 12, 1547–1558, doi:10.1109/TVCG.2006.97.
80. Stained Glass Window Generator Available online: <https://deepai.org/machine-learning-model/stained-glass-generator> (accessed on 28 May 2025).

Disclaimer/Publisher’s Note: The statements, opinions and data contained in all publications are solely those of the individual author(s) and contributor(s) and not of MDPI and/or the editor(s). MDPI and/or the editor(s) disclaim responsibility for any injury to people or property resulting from any ideas, methods, instructions or products referred to in the content.